Graphical Abstract

To create your abstract, type over the instructions in the template box below.
Fonts or abstract dimensions should not be changed or altered.

The endocyclic oxygen atom of D-manno-pyranose is involved in its binding to pradimicins

Yasunori Watanabe, Fumiya Yamaji, Makoto Ojika, Takahiro Sugawara, Dai Akase, Misako Aida, Yasuhiro Igarashi, Yukishige Ito, Yu Nakagawa

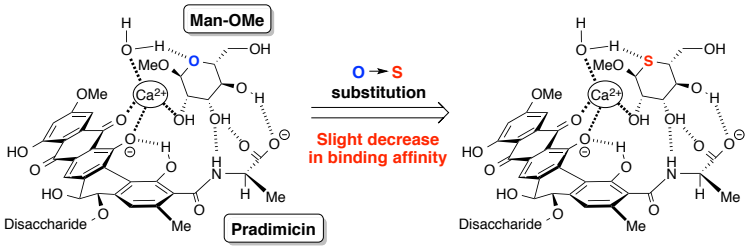

Tetrahedron Letters
journal homepage: www.elsevier.com

The endocyclic oxygen atom of D-mannopyranose is involved in its binding to pradimicins

Yasunori Watanabe[a] , Fumiya Yamaji[a], Makoto Ojika[a], Takahiro Sugawara[b], Dai Akase[b], Misako Aida[b], Yasuhiro Igarashi[c], Yukishige Ito[d], Yu Nakagawa[a,d,*]

[a]*Department of Applied Biosciences, Graduate School of Bioagricultural Sciences, Nagoya University, Furo-cho, Chikusa-ku, Nagoya 464-8601, Japan*
[b]*Center for Quantum Life Sciences, and Department of Chemistry, Graduate School of Science, Hiroshima University, 1-3-1 Kagamiyama, Higashi-Hiroshima, Hiroshima 739-8526, Japan*
[c]*Biotechnology Research Center, Toyama Prefectural University, 5180 Kurokawa, Imizu, Toyama 939-0398, Japan*
[d]*Synthetic Cellular Chemistry Laboratory, RIKEN, 2-1 Hirosawa, Wako, Saitama 351-0198, Japan*

ARTICLE INFO

Article history:
Received
Received in revised form
Accepted
Available online

Keywords:
Antibiotic
Carbohydrate recognition
Molecular interaction
Pradimicin

ABSTRACT

Methyl 5-thio-α-D-mannopyranoside (**1**) and six inositols were evaluated for their ability to bind to pradimicins (PRMs) *via* molecular modeling and three binding assays. In all the experiments, the binding affinity of **1** was slightly lower than that of methyl α-D-mannopyranoside (Man-OMe) and inositols hardly bound to PRMs. These results indicate that the endocyclic oxygen atom of Man-OMe is involved in its binding to PRMs.

Introduction

Pradimicins (PRMs, Fig. 1) [1–3] are a unique class of antibiotics that show anti-fungal, antiviral, and anti-parasitic activities by binding to the glycans of pathogenic species [4–8]. Their glycan binding ability originates from specific interactions with D-mannose (Man) in the presence of Ca^{2+}. Since such C-type lectin-like behavior is never observed in any other small molecule, considerable attention has been directed towards the molecular basis of Man recognition by PRMs. Earlier studies suggested that PRMs bind Man in Ca^{2+}-containing neutral solutions to form insoluble aggregates of the ternary [$PRM_2/Ca^{2+}/Man_4$] complex [9]. Subsequent spectroscopic analysis showed that PRMs initially form the binary [PRM_2/Ca^{2+}] complex, which subsequently binds four molecules of Man in two independent steps (Scheme 1) [10–12]. However, during the two decades since the discovery of PRMs, the aggregate-forming propensity of the [$PRM_2/Ca^{2+}/Man_2$] and [$PRM_2/Ca^{2+}/Man_4$] complexes has hampered their structural analysis, leaving the question as to how PRMs bind Man unanswered.

Recognizing this issue, our group started, in 2009, to explore an analytical strategy based on solid-state NMR technology [13–15]. Making use of the inherent aggregate-forming property of PRM-A (Fig. 1) [2], the first member of PRMs, we prepared solid aggregates mainly composed of a 1:1 complex of PRM-A and methyl α-D-mannopyranoside (Man-OMe), i.e. the [PRM-A_2/Ca^{2+}/Man-OMe_2] complex. Structural analysis by dipolar-assisted rotational resonance (DARR) revealed that the anthraquinone and D-alanine moieties of PRM-A are in close contact with the C2 and C3 positions of Man-OMe, respectively, in the complex [15]. Recently, we also determined the crystal structure of the [PRM_2/Ca^{2+}] complex using a water-soluble PRM derivative [16]. Based on these findings, we performed density functional theory (DFT) calculations to estimate the structure of the [PRM-A_2/Ca^{2+}/Man-OMe_2] complex (Fig. 1). In our binding model, the 2-, 3-, and 4-hydroxyl groups of Man-OMe are involved in Ca^{2+} coordination and/or hydrogen bonding with PRM-A, while the 1-methoxy and 6-hydroxyl groups do not interact with either Ca^{2+} or PRM-A. The endocyclic oxygen atom in the pyranose ring of Man-OMe acts as an acceptor for hydrogen bonding with the Ca^{2+}-coordinated water molecule.

The roles of the hydroxyl groups of Man-OMe in our binding model are in good agreement with our previous finding that PRM-A binds 6-deoxy-Man-OMe but not with 2-, 3-, and 4-deoxy-Man-OMe [15]. Regarding its 1-methoxy group, Man and β anomer of Man-OMe were found to co-precipitate with PRM-A in a manner similar to Man-OMe [17], supporting the trivial role of the methoxyl group and configuration at the C1 position of Man-OMe. However, there is a lack of experimental evidence to support the involvement of the endocyclic oxygen atom of Man-OMe in binding to PRM-A. In this study, we evaluated binding of PRMs with methyl 5-thio-α-D-mannopyranoside (**1**, Fig. 1) [18] to examine the role of the endocyclic oxygen atom of Man-OMe. We also revealed that PRMs are insensitive to six inositols, which mimic the spatial configuration of the 2-, 3-, and 4-hydroxyl groups of Man while lacking an endocyclic oxygen atom.

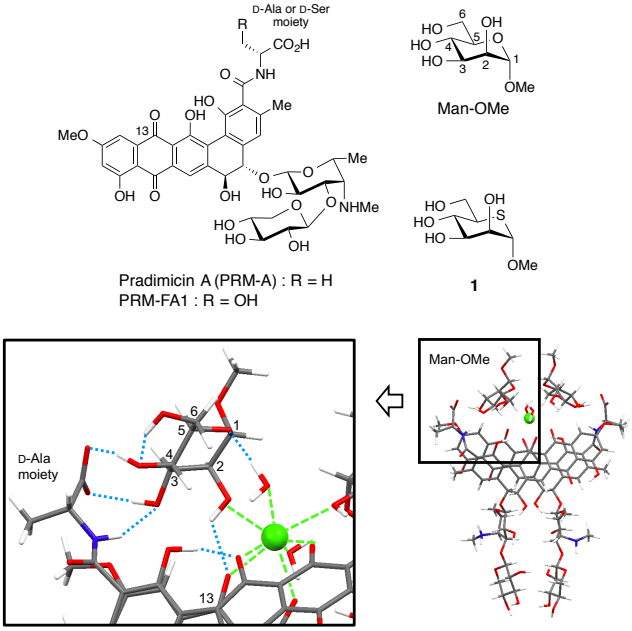

Figure 1. Structures of pradimicins, Man-OMe, and **1** (upper) and energy-minimized structure of the [PRM-A_2/Ca^{2+}/Man-OMe_2] complex obtained by solid-state NMR analysis and DFT calculations at the ω-B97X-D/6-31G(d) level of theory (lower). Carbon, oxygen, nitrogen, hydrogen, and calcium atoms are shown in gray, red, blue, white, and green, respectively. Blue and green dotted lines represent possible hydrogen bonding and Ca^{2+} coordination, respectively. Two water molecules are coordinated to Ca^{2+} in the complex.

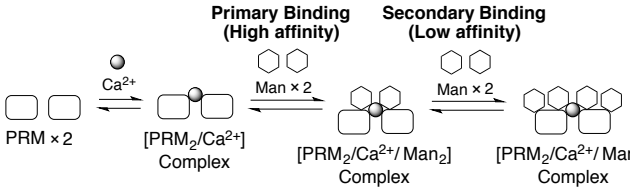

Scheme 1. Complex-forming process of PRM with Ca^{2+} ion and Man.

Results and discussion

The binding evaluation of PRMs with **1** started with DFT studies centered on estimating the effect of the sulfur atom on our proposed binding model. An initial structure was constructed for the [PRM-A_2/Ca^{2+}/**1**$_2$] complex by replacing Man-OMe with **1**, followed by optimization through DFT calculations at the ωB97X-D/6-31G(d) level of theory. The obtained energy-minimized structure (Fig. 2) shows a remarkable similarity to the [PRM-A_2/Ca^{2+}/Man-OMe_2] complex in terms of the hydrogen-bond network and Ca^{2+} coordination. The 2-hydroxyl group of **1** is involved in both Ca^{2+} coordination and hydrogen bonding with the 13-carbonyl group of PRM-A, and the 3- and 4-hydroxyl groups interact with the D-alanine moiety of PRM-A. Moreover, a hydrogen bond is also found between the Ca^{2+}-coordinated water molecule and the endocyclic sulfur atom of **1**, suggesting that **1** could behave similarly to Man-OMe in binding to PRM-A.

Next, we calculated the interaction energy (ΔE) between the [PRM-A_2/Ca^{2+}] complex and Man-OMe or **1**. For interaction energies, BSSE (basis set superposition error) was taken into consideration. The ΔE value for **1** was –139.96 kcal/mol, while that for Man-OMe was –144.30 kcal/mol. The absolute value of ΔE for **1** is slightly smaller than that for Man-OMe, implying a lower binding affinity of **1**. The main reason for this is the weak interaction of the endocyclic sulfur atom of **1** with the Ca^{2+}-coordinated water molecule, compared with that of the corresponding oxygen atom of Man-OMe. These results of our preliminary calculations collectively suggest that **1** would bind to the [PRM_2/Ca^{2+}] complex in a manner similar to PRM-A, but with lower potency.

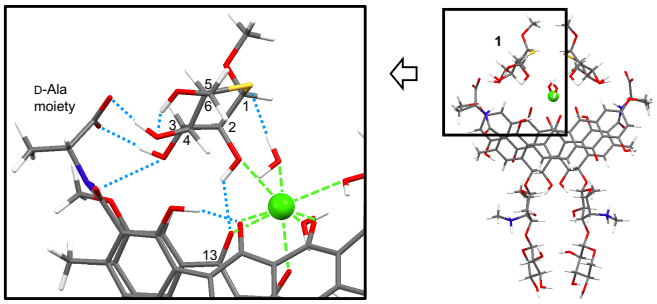

Figure 2. Energy-minimized structure of the [PRM-A_2/Ca^{2+}/**1**$_2$] complex obtained by DFT calculations at the ω-B97X-D/6-31G(d) level of theory. Carbon, oxygen, nitrogen, sulfur, hydrogen, and calcium atoms are shown in gray, red, blue, yellow, white, and green, respectively. Blue and green dotted lines represent possible hydrogen bonding and Ca^{2+} coordination, respectively. Two water molecules are coordinated to Ca^{2+} in the complex.

As the first validation of our computational prediction, we attempted to determine a binding constant for **1** to PRM-A by isothermal titration calorimetry (ITC). However, unfortunately, complex formation of PRM-A with **1** caused severe aggregation, resulting in complicated ITC signals. We, therefore, performed co-precipitation experiments [17] as an alternative evaluation. Our established procedure consists of four steps: (1) aggregate formation of PRM-A with $CaCl_2$ and sugars in aqueous solutions at pH 6.0, (2) extensive washing of the aggregate, (3) acid treatment to dissociate the aggregate, and (4) quantification of the sugar/PRM-A molar ratio by ^{1}H-NMR on the basis of their integration values. Since step (2) involves the complete release of sugars from the secondary binding site of the [PRM-A_2/Ca^{2+}] complex, this co-precipitation experiment can quantify the primary binding of sugars (Scheme 1). Table 1 shows the **1**/PRM-A molar ratio in the aggregate, along with those for Man-OMe and methyl α-D-glucopyranoside (Glc-OMe). While only a negligible amount of Glc-OMe was detected in the aggregate, **1** showed significant binding to PRM-A. However, the detected amount of **1** was slightly lower than that of Man-OMe. This result reflects lower affinity of **1** than that of Man-OMe, supporting our modeling study.

To obtain more experimental support, we evaluated the antagonistic effects of **1** on the antifungal activity of PRM-A against *Candida rugosa* (MIC of PRM-A = 4 μg/mL). Earlier studies revealed that the antifungal activity of PRM-A is closely related to its binding to cell wall mannans and is suppressed by the exogenous addition of oligomannoses [9]. Thus, we determined the minimum antagonistic concentrations (MACs) of Man-OMe, Glc-OMe, and **1** required for suppressing the PRM-A (32 μg/mL)-induced growth inhibition of *C. rugosa* cells. As shown in Table 2, Man-OMe exerted a significant antagonistic effect, while Glc-OMe did not suppress the antifungal activity of PRM-A up to a 64

mM concentration. Mirroring the results of the co-precipitation experiments, the MAC value of **1** was slightly higher than that of Man-OMe, supporting weaker binding of **1** to PRM-A compared with that of Man-OMe.

Table 1.
Molar ratio of Man-OMe, Glc-OMe, **1**, and inositols relative to PRM-A in aggregates.

Sugar	Sugar/PRM-A ratio
Man-OMe	1.02 (0.05)[a]
Glc-OMe	< 0.01
1	0.85 (0.01)
myo-Inositol	< 0.01
allo-Inositol	< 0.01
epi-Inositol	< 0.01
1D-Inositol	< 0.01
1L-Inositol	< 0.01
muco-Inositol	< 0.01

[a] Standard deviation of at least three separate experiments.

Table 2.
Antagonistic effect of Man-OMe, Glc-OMe, **1**, and inositols on antifungal activity of PRM-A against *Candida rugosa*.

Sugar	MAC[a] (mM)
Man-OMe	16
Glc-OMe	> 64
1	32
myo-Inositol	> 64
allo-Inositol	> 64
epi-Inositol	> 64
1D-Inositol	> 64
1L-Inositol	> 64
muco-Inositol	> 64

[a] Minimum antagonistic concentration required for suppressing PRM-A (32 μg/mL)-induced growth inhibition of *C. rugosa* cells. The experiments were performed as duplicates.

Further experimental support was obtained by aggregation experiments using PRM-FA1 (Fig. 1), a D-serine analog of PRM-A [19]. Unlike the [PRM-A_2/Ca^{2+}] complex, the [PRM-$FA1_2$/Ca^{2+}] complex hardly aggregates in neutral aqueous solutions. However, when it binds Man, the resulting [PRM-$FA1_2$/Ca^{2+}/Man_2] and [PRM-$FA1_2$/Ca^{2+}/Man_4] complexes easily aggregate to produce precipitates. Assuming that the aggregability of PRM-FA1 depends on its binding affinity for sugars, we evaluated the binding affinities of Man-OMe, Glc-OMe, and **1** by measuring their concentrations (AC_{50}) that induce 50% aggregation of PRM-FA1 (Table 3). Similar to the results obtained in the above two tests using PRM-A, **1** induced the aggregation of PRM-FA1, but with less potency than that of Man-OMe. Inertness of PRM-FA1 towards Glc-OMe suggests that its aggregation truly originates from the specific binding of Man-OMe or **1**. Taken together, all the three abovementioned experiments support our computational prediction, and thereby validate our binding model, in which the endocyclic oxygen atom of Man is involved in its binding to PRMs.

These results further led us to predict that PRMs would be insensitive to inositols, which mimic the spatial configuration of 2-, 3-, and 4-hydroxyl groups of Man while lacking the endocyclic oxygen atom (Fig. 3). To confirm this assumption, six inositols were evaluated for their binding to PRM-A and PRM-FA1. Results are shown in Tables 1–3. As expected, these inositols exhibited negligible binding in all three binding experiments. These results indicate that PRMs can discriminate Man not only from common monosaccharides but also from inositols.

Table 3.
Aggregate formation of PRM-FA1 induced by Man-OMe, Glc-OMe, **1**, and inositols.

Sugar	AC_{50}[a] (mM)
Man-OMe	5.8
Glc-OMe	> 10
1	6.8
myo-Inositol	> 10
allo-Inositol	> 10
epi-Inositol	> 10
1D-Inositol	> 10
1L-Inositol	> 10
muco-Inositol	> 10

[a] Concentration that induces 50% aggregation of PRM-FA1. AC_{50} values were determined from corresponding dose-response curves (see ESI).

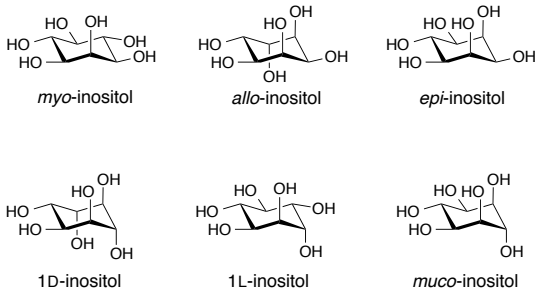

Figure 3. Structures of inositols used in this study.

In summary, we evaluated the binding of methyl 5-thio-α-D-mannopyranoside (**1**) to PRMs through molecular modeling and three binding experiments. The results collectively indicate that **1** binds to PRMs with slightly lower affinity than Man-OMe, supporting our binding model, in which the endocyclic oxygen atom of Man-OMe participates in binding to PRMs. Additionally, we demonstrated that PRMs hardly form a ternary complex with inositols, although they have a spatial configuration mimicking that of the 2-, 3-, and 4-hydroxyl groups of Man. This emerging selectivity for Man over inositols further underscores the potential of PRMs as superior lectin mimics. Investigation into the medicinal and glycobiological applications of PRMs is underway, and its results will be reported in due course.

Acknowledgments

This work was partly supported by a Grant-in-Aid for JSPS Fellow (No. 17J03048) and JSPS KAKENHI Grant (No. JP15H04496). *Candida rugosa* AJ 14513 (NBRC 0750) was provided from Ajinomoto Co., Inc. (Kanagawa, Japan). The DFT calculations were partly carried out at the Research Center for Computational Science, Okazaki, Japan. We thank Mr. Kazushi Koga for NMR spectroscopic assistance.

Appendix A. Supplementary data

Supplementary data to this article can be found online at https://xxxx.

References

[1] T. Takeuchi, H. Hara, H. Naganawa, M. Okada, M. Hamada, H. Umezawa, S. Gomi, M. Sezaki, S. Kondo, J. Antibiot. 41 (1988) 807–811.
[2] T. Oki, M. Konishi, K. Tomatsu, K. Tomita, K. Saitoh, M. Tsunakawa, M. Nishio, T. Miyaki, H. Kawaguchi, J. Antibiot. 41 (1988) 1701–1704.
[3] Y. Fukagawa, T. Ueki, K. Numata, T. Oki, Actinomycetologia 7 (1993) 1–22.
[4] M.M.F. Alen, T.D. Burghgraeve, S.J.F. Kaptein, J. Balzarini, J. Neyts, D. Schols, PLoS ONE 6 (2011) e21658.
[5] J. Balzarini, Nat. Rev. Microbiol. 5 (2007) 583–597.
[6] V.M. Castillo-Acosta, L.M. Ruiz-Pérez, J. Etxebarria, N.C. Reichardt, M. Navarro, Y. Igarashi, S. Liekens, J. Balzarini, D. González-Pacanowska, PLoS Pathog. 12 (2016) e1005851.
[7] K.O. François, J. Balzarini, Med. Res. Rev. 32 (2012) 349–387.
[8] Y. Igarashi, T. Oki, Adv. Appl. Microbiol. 54 (2004) 147–166.
[9] T. Ueki, K. Numata, Y. Sawada, T. Nakajima, Y. Fukagawa, T. Oki, J. Antibiot. 46 (1993) 149–161.
[10] M. Hu, Y. Ishizuka, Y. Igarashi, T. Oki, H. Nakanishi, Spectrochim. Acta A 55 (1999) 2547–2558.
[11] M. Hu, Y. Ishizuka, Y. Igarashi, T. Oki, H. Nakanishi, Spectrochim. Acta A 56 (1999) 181–191.
[12] K. Fujikawa, Y. Tsukamoto, T. Oki, Y.C. Lee, Glycobiology 8 (1998) 407–414.
[13] Y. Nakagawa, Y. Masuda, K. Yamada, T. Doi, K. Takegoshi, Y. Igarashi, Y. Ito, Angew. Chem. Int. Ed. 50 (2011) 6084–6088.
[14] Y. Nakagawa, T. Doi, Y. Masuda, K. Takegoshi, Y. Igarashi, Y. Ito, J. Am. Chem. Soc. 133 (2011) 17485–17493.
[15] Y. Nakagawa, T. Doi, K. Takegoshi, Y. Igarashi, Y. Ito, Chem. Eur. J. 19 (2013) 10516–10525.
[16] Y. Nakagawa, T. Doi, K. Takegoshi, T. Sugahara, D. Akase, M. Aida, K. Tsuzuki, Y. Watanabe, T. Tomura, M. Ojika, Y. Igarashi, D. Hashizume, Y. Ito, Cell Chem. Biol. 26 (2019) 950–959.
[17] Y. Nakagawa, Y. Watanabe, Y. Igarashi, Y. Ito, M. Ojika, Bioorg. Med. Chem. Lett. 25 (2015) 2963–2966.
[18] M. Izumi, Y. Suhara, Y. Ichikawa, J. Org. Chem. 63 (1998) 4811–4816.
[19] Y. Sawada, M. Hatori, H. Yamamoto, M. Nishio, T. Miyaki, T. Oki, J. Antibiot. 43 (1990) 1223–1229.